Materials Science and Engineering A 410–411 (2005) 381–385

www.elsevier.com/locate/msea

Effect of processing route and second phase particles on grain refinement during equal-channel angular extrusion

M. Berta [a], P.J. Apps [b], P.B. Prangnell [a,*]

[a] *Manchester Materials Science Centre, The University of Manchester, Grosvenor Street, Manchester M1 7HS, UK*
[b] *Health and Safety Laboratory, Broad Lane, Sheffield S3 7HQ, UK*

Received in revised form 11 April 2005

Abstract

The effect of coarse and fine second-phase particles on the formation of ultra-fine grained (UFG) structures have been compared during severe deformation by equal-channel angular extrusion using routes A (no rotation) and B_C (+90° rotation). The presence of coarse particles has been found to increase the rate of grain refinement with route A and the homogeneity of the submicron grain structure formed, but appears less effective using route B_C. In contrast, the presence of fine dispersoids inhibits the development of new high-angle grain boundaries and the formation of an UFG structure with both routes. Retardation is far more pronounced with rotation of the sample and the dispersiod-containing alloy processed by route B_C contained mainly subgrains. The mechanisms operating in each case are discussed.

Keywords: ECAE; Severe deformation; Grain refinement; Particles; Dispersiods; Processing route

1. Introduction

Equal channel angular extrusion (ECAE) is now a well-established method of processing metals to ultra-high strains, and has seen considerable research interest over the last decade (e.g. [1–5]). It has been frequently demonstrated that severe deformation by ECAE to strains of the order of 10 can produce submicron grain structures in metallic alloys [1–5]. Although much research has been conducted on the nature of the grain structures of severely deformed alloys [1–5], and more recently on the evolution of the deformation structure to ultra-high strains [2–5], there is still some debate about the effects of the processing route and the mechanisms of grain refinement. For example, it has been found that rotation of the billet by 90° between each extrusion cycle can increase, or reduce, the level of grain refinement, depending on the die angle, die corner profile and material [2,6–8]. To date, the role of the material variables have not been systematically considered in this context. In previous work it has been shown that, during ECAE processing without rotation of the billet, second phase particles can have a very important effect on the rate and level of grain refinement achieved [9,10]. Coarse micrometer-scale particles were found to accelerate the rate of grain refinement by generating new high angle boundaries within their deformation zones and from particle simulated deformation bands [9], whereas nanometer scale dispersiods can retard the rate of grain refinement by homogenising the slip [10]. Methods of reducing the strain required to form an ultra-fine grained (UFG) material, such as exploiting the use of coarse particles, are clearly of industrial importance, while in many cases fine dispersiods are required in an UFG material to stabilise the grain structure for subsequent applications, such as superplastic forming.

In this paper new results are presented on the effect of coarse particles and fine dispersiods on the level of grain refinement and homogeneity of the sub micrometer grain microstructure that can be produced during ECAE processing with billet rotation, using route B_C (+90°). The results are compared to data, obtained using the same simple model alloys without billet rotation (route A).

2. Experimental

Three alloys: 8079 (Al–1.3 wt.% Fe–0.09 wt.% Si), Al–0.2 wt.% Sc and Al–0.1 wt.% Mg, were deformed by ECAE at room temperature by 15 extrusion cycles to a Von Mises strains

* Corresponding author. Tel.: +44 161 200 2610; fax: +44 161 200 3586.
E-mail address: philip.prangnell@umist.ac.uk (P.B. Prangnell).

0921-5093/$ – see front matter © 2005 Elsevier B.V. All rights reserved.
doi:10.1016/j.msea.2005.08.026

of ∼10. A die angle of 120° was used with a sharp die corner. Processing was carried out without rotation (Route A) and with rotation by 90° (Route B_C) between each extrusion cycle. Prior to deformation, the 8079 and Al–0.2Sc alloys were heat treated to develop a uniform distribution of second phase particles (see references [9,10]). All the materials had a similar initial grain size of ∼300 μm. The 8079 and Al–0.2Sc alloys contained coarse θ ($Al_{13}Fe_4$) particles and fine coherent Al_3Sc dispersiods, with diameters of ∼2 and ∼20 nm and an interparticle spacings of the order of 10 and 100 nm, respectively. The high-purity single-phase Al–0.1% Mg alloy was used as a control material. The material's deformation structures were characterized using samples taken from the centre of the of the ECAE billet in the ND–ED plane, by high-resolution EBSD using a FEGSEM fitted with HKL technology EBSD system. The spatial and angular resolution of the system were >50 nm and ∼1°, respectively. A low misorientation cut-off of 1.5° was used to minimise misorientation noise. Low angle boundaries (LABs) have been defined as having between 1.5° and 15° misorientations and high angle grain boundaries (HAGBs) greater than 15° misorientation (depicted as black and light grey lines).

3. Results and discussion

3.1. Severe deformation by route A

The microstructures of the three materials processed by route A are shown in EBSD maps in Fig. 1. More detailed descriptions can be found in [2–4,9,10]. Here, their main features are summarised after deformation to an effective strain of ∼10 (15 ECAE passes) for comparison purposes with route B_C. After this ultra-high strain deformation all three alloys mainly contained submicron grains structures with a high fraction of HAGBs (Fig. 1a and b). The grain structures tended to be fibrous, elongated in the extrusion direction, and develop from a 'lamellar' HAGB structure seen at lower strains [2–4]. Overall the grain structures appear reasonably similar, but there are significant differences between the three materials.

Statistical analysis of the percentage HAGB area, mean boundary misorientations and grain sizes are shown in Table 1, from over 5000 grains. The grain sizes have also been measured using the mean linear intercept method parallel and perpendicular to the main direction of HAGB alignment and from the equivalent circular diameter (ECD) after grain reconstruction from the EBSD data. The ECD data has also been used to determine the width of the grain size distributions from the standard deviation normalised with respect to the distribution average. It should be noted that the grain length linear intercept (λ_y) is unreliable with aligned SMG microstructures because the retained longer fibrous grains are frequently bent and do not all align perfectly with the reference frame. Nevertheless, the 8079 alloy, which contains coarse second phase particles, had the most uniform and consistently lowest aspect ratio submicrometer grain structure. It also had the lowest level of retained larger fibrous grains and lowest fraction of low angle boundaries of less than 15° in misorientation (%HAGBs ∼85%; Table 1) as well as the highest average boundary misorientation. In comparison, the dispersiod-containing alloy had the most retained fibrous grain fragments (arrowed), lowest fraction of HAGBs (64%; Table 1), and the largest grain size, while the single-phase alloy lay somewhere in between (74% HAGBs). The dispersiod-containing alloy also had the widest grain size distribution, reflecting the higher frequency of larger retained fibrous grain fragments.

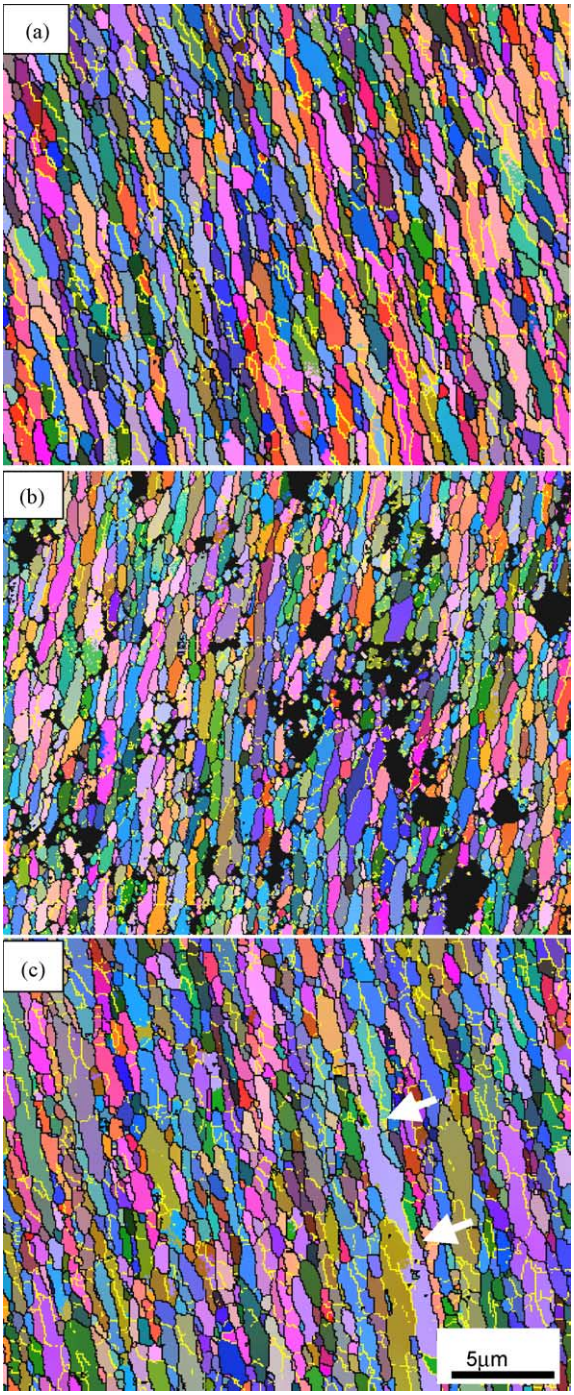

Fig. 1. Example EBSD maps of the three model alloys deformed to an effective strain of 10 by route A: (a) the single phase alloy Al–0.13% Mg, (b) the coarse particle containing 8079 and (c) the Al–0.2% Sc alloy with fine dispersoids.

Table 1
Average statistical data of the three model alloys determined from the EBSD maps after deformation to an effective strain of 10 by route A and B_C from measurements on ~5000 grains

Route: material	Mean grain size (μm)					HAGBs	Misorientation
	λ_x	λ_y	λ_x/λ_y	ECD	$\sigma_{S.D.}/d_m$		
A: Al–0.13 Mg	0.48	0.85	1.8	0.87	0.72	74	31°
A: 8079	0.36	0.49	1.4	0.6	0.71	85	35°
A: Al–0.2Sc	0.73	2.2	3.0	0.89	1.39	64	27°
B_C: Al–0.13Mg	0.89	0.93	1.1	0.91	0.89	71	29°
B_C: 8079	0.63	0.92	1.4	0.78	0.74	65	28°
B_C: Al–0.2Sc	2.4	5.4	2.3	1.3	1.84	46	19°

Showing the grain sizes obtained, using the mean linear intercept, λ_x, parallel and, λ_y, perpendicular to the main direction of HAGB alignment, grain aspect ratio, equivalent circular diameter (ECD) grain size after grain reconstruction from the EBSD data, the standard deviation of the ECD grain size distributions normalised with respect to the mean diameter ($\sigma_{S.D.}/d_m$), the percentage of HAGB area, and the mean boundary misorientations.

3.2. Severe deformation by Route B_C

EBSD maps of the three model alloys after deformation to an effective strain of ~10 (15 ECAE passes) with 90° rotation between each extrusion cycle are shown in Fig. 2. The deformation structures are aligned with the shear direction from the last extrusion cycle. If these maps are compared to those without rotation, it is immediately apparent that the differences between the three alloys are much more obvious. In the case of the single-phase alloy, although grains are more equiaxed, a more heterogeneous microstructure is seen than for route A, comprised of a mixture of bands of ultra-fine grains and coarser grain fragments containing mainly subgrains (arrow Fig. 2a). Overall this leads to a slightly larger average grain size and lower fraction of HAGBs than for route A (Table 1). There is also a wider spread in the normalised grain size distribution, reflecting the mixture of bands of very fine and coarse unrefined regions. The LAGBs within the coarser grain fragments have significant misorientations of ~5°, and are therefore well-defined subgrains, which could easily be mistaken as grains in the TEM. In comparison the coarse particle containing alloy, 8079, appears to have a more homogeneous grain structure, but again contains unrefined regions comprised of low aspect ratio submicron grains, which tend to be smaller than in the single-phase alloy. The statistical data in Table 1 show that this alloy is more significantly less refined than when processed by route A.

Much more surprising are the results for the dispersiod containing Al–0.2% Sc alloy processed by route B_C, which, with a HAGB fraction of 46%, is predominantly comprised of subgrains and cannot be described as containing a sub micrometer grain structure. The average 'grain size measurements' for this alloy in Table 1 are therefore somewhat misleading, but are substantially larger than for any of the other samples. The average boundary misorientation for this material was only 19°. The deformation structure contained a few isolated bands of sub micrometer grains, as well as deformation bands, delineated by higher misorientation HAGBs, whereas the LAGB misorientations of the subgrains within such bands were predominantly around ~3–6°. The grain refinement process for this material was already found to be inhibited using route A [10], but with route B_C the rate of formation of new HAGB area has clearly been much more significantly affected by the presence of a high density of fine dispersiod particles.

3.3. Comparison of the grain refinement behaviour of the alloys and processing routes

Although there is still some debate as to how best to represent the deformation within the dies process zone, when a material is deformed by ECAE without rotation of the billet, an element is observed to be continuously sheared, leading to pre-existing boundaries becoming rotated and elongated towards the extrusion direction forming a fibrous deformation structure. In the single-phase Al–0.1% Mg alloy, the deformation structure evolution during ECAE processing by route A has already been reported [2–4,9,10]. At low strains dislocations dynamically recover into a banded cellular structure divided by low misorientation subgrain boundaries. The dense dislocation walls that delineate the cell bands are frequently found to be parallel to the dies plane of intersection, or principal shear plane and are thus probably transient features which are destroyed and reform each cycle. Unstable grains are also subdivided on a coarse scale by the formation of deformation bands. Further deformation leads to the formation of micro-shear bands, due to instability in plastic flow. The new HAGBs formed by these microshear bands and the initial grain and deformation band boundaries are permanent and rotate and align in the deformation direction. Their spacing becomes compressed with strain until they form a fine lamellar HAGB structure, which breaks up to give the submicron-grained structure produced at ultra-high strains.

In the case of deformation by route B_C, which involves shear on alternate planes, the net strain is redundant and an element returns to its original shape every four cycles. This means that any pre-existing HAGBs do not necessarily extend in area, or compress in spacing, with accumulated strain. The mechanisms by which grain refinement occurs under these conditions are still poorly understood, but are believed to be predominantly due to new HAGBs being generated from shear bands. These are promoted by route B_C due to instability in flow being encouraged by the reorientation of the shear direction relative to the original principal direction of alignment of dense dislocation boundaries formed in previous cycles [2].

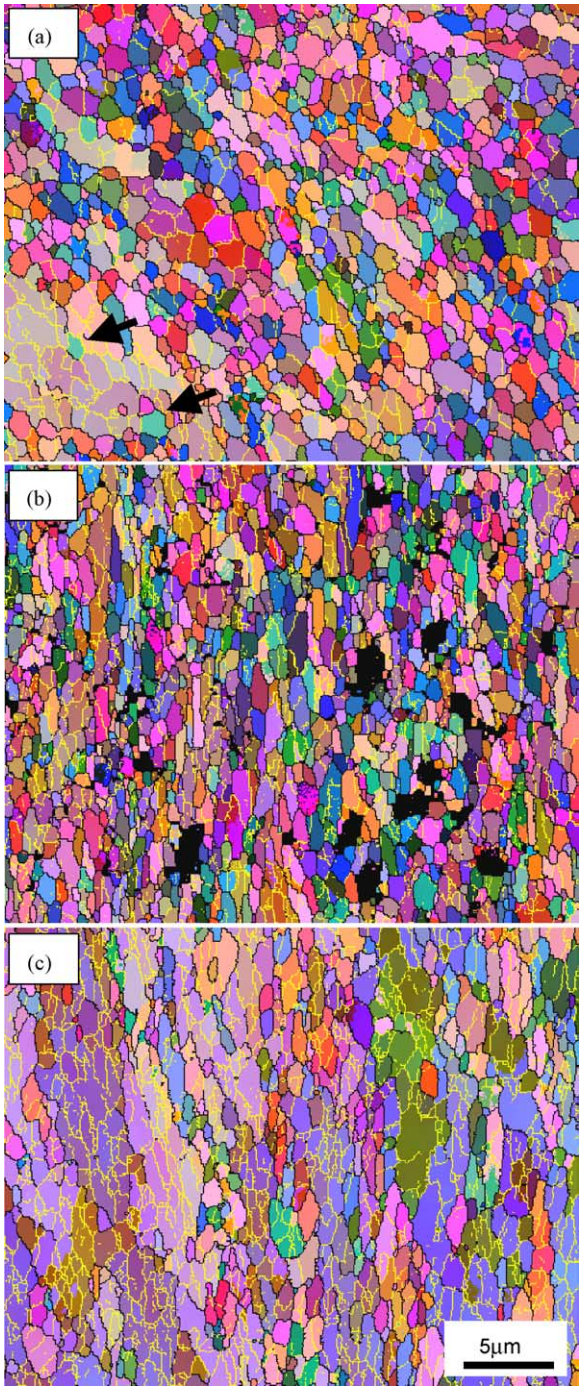

Fig. 2. Example EBSD maps of the three model alloys deformed to an effective strain of 10 by route B_C (+90° rotation): (a) the single phase alloy Al–0.13% Mg, (b) the coarse particle containing 8079 and (c) the Al–0.2% Sc alloy with fine dispersoids.

This leads to the heterogeneous deformation structures seen in Fig. 2a, comprised of bands of fine grains in regions of high local strain formed by shear bands and retained islands of subgrains.

In a coarse particle containing alloy like 8079, the generation of high angle grain boundaries, in local deformation zones around coarse second-phase particles and particle stimulated deformation bands leads to the rapid formation of new HAGBs on the scale of the inter-particle spacing [9]. This, combined with heterogeneous plastic flow around the particles, which breaks up lamellar deformation structures at higher strains, has been found to lead to the formation of a uniform submicron grained structures at much lower strains than in the single phase alloy processed by route A [9]. The formation of deformation zones around coarse hard particles and the refinement of the spacing of deformation bands may also be beneficial for producing an ultra-fine grain structure more rapidly by route B_C, but the comparative rate of grain refinement at low strains has not yet been investigated. In contrast, intense shear bands will be less likely to develop in the particle-containing alloy, as the slip line length will be reduced to the interparticle spacing and this may explain the differences observed in Table 1.

With route A the level of grain refinement was considerably reduced in the dispersoid-containing alloy, compared to a single phase alloy using route, but was far more significantly affected when processed by route B_C. During processing by route A, it has been found that the presence of a high density of Al_3Sc dispersoids inhibits both the formation of cells and sharp DDWs, which define the cell band structures seen at moderate strains in single-phase alloys [10]. The more weakly misorientated and diffuse dislocation boundaries present in the dispersoid-containing alloy, plus the general homogenisation of slip by the dispersoids, prevents the formation of microshear bands which blocks this important mechanism of HAGB formation. The main source of new HAGB area in the dispersoid containing alloy at low to medium strains is therefore mainly restricted to the formation of coarse deformation bands by texture-orientation instability, and the extension of these, and the original grain boundaries due to the geometric shape change of an element with strain. This in turn delays the formation of a lamellar HAGB structure and the development of a uniform submicron grained material at ultra-high strains. In the case of processing with rotation of the billet, there is no net geometric shape change of an element to reduce the HAGB separation with strain and by reducing the tendency for the formation of shear bands, which is the main mechanism of grain subdivision with this processing route, the finely spaced dispersiods appear to have a more dramatic effect on inhibiting grain refinement.

4. Conclusions

The effect of coarse and fine second-phase particles on the formation of ultra-fine grain structures by ECAE have been compared using the two processing routes A and B_C. The presence of coarse particles has been found to increase the rate of grain refinement and the homogeneity of the submicron grain structure formed using route A, due, but appears less effective with route B_C. In contrast, the presence of fine particles inhibits the development of new high-angle grain boundaries and the formation of a fine grain structure, by both processing routes, but this effect is much more pronounced using route B_C. This behaviour is believed to be caused by the dispersiods homogenising slip and inhibiting the formation of shear bands during deformation.

References

[1] R.Z. Valiev, R.K. Islamgaliev, I.V. Alexandrov, Prog. Mater. Sci. 45 (2000) 103.
[2] P.B. Prangnell, J.R. Bowen, A. Gholinia, in: A.R. Dinesen, et al. (Eds.), Proceedings of 22nd Risø International Symposium on Science of Metastable and Nanocrystalline Alloys, Risø National Laboratory, Roskilde Denmark, 2001, p. 105.
[3] P.B. Prangnell, J.R. Bowen, in: Y.T. Zhu, et al. (Eds.), Proceedings of Second International Symposium on Ultra-Fine Grained Materials, TMS, Warrendale, PA, USA, 2002, p. 89.
[4] P.B. Prangnell, J.R. Bowen, P.J. Apps, Mater. Sci. Eng. 375–377A (2003) 178.
[5] F. Dalla Torre, R. Lapovok, J. Sandlin, P.F. Thomson, C.H.J. Davies, E.V. Pereloma, Acta Mater. 52 (2004) 4819.
[6] A. Gholina, P.B. Prangnell, M.V. Markushev, Acta Mater. 48 (2000) 1115.
[7] Y. Iwahashi, Z. Horita, M. Nemoto, T.G. Langdon, Acta Mater. 45 (1997) 4733.
[8] l. Dupy, E.F. Rauch, Mater. Sci. Eng. A337 (2002) 241.
[9] P.J. Apps, J.R. Bowen, P.B. Prangnell, Acta Mater. 51 (2003) 2811.
[10] P.J. Apps, M. Berta, P.B. Prangnell, Acta Mater. 53 (2004) 49.